

Determination of the Λ_c^+ spin via the reaction $e^+e^- \rightarrow \Lambda_c^+ \bar{\Lambda}_c^-$

M. Ablikim¹, M. N. Achasov^{10,c}, P. Adlarson⁶⁴, S. Ahmed¹⁵, M. Albrecht⁴, A. Amoroso^{63A,63C}, Q. An^{60,48}, Anita²¹, Y. Bai⁴⁷, O. Bakina²⁹, R. Baldini Ferroli^{23A}, I. Balossino^{24A}, Y. Ban^{38,k}, K. Begzsuren²⁶, J. V. Bennett⁵, N. Berger²⁸, M. Bertani^{23A}, D. Bettoni^{24A}, F. Bianchi^{63A,63C}, J. Biernat⁶⁴, J. Bloms⁵⁷, A. Bortone^{63A,63C}, I. Boyko²⁹, R. A. Briere⁵, H. Cai⁶⁵, X. Cai^{1,48}, A. Calcaterra^{23A}, G. F. Cao^{1,52}, N. Cao^{1,52}, S. A. Cetin^{51B}, J. F. Chang^{1,48}, W. L. Chang^{1,52}, G. Chelkov^{29,b}, D. Y. Chen⁶, G. Chen¹, H. S. Chen^{1,52}, M. L. Chen^{1,48}, S. J. Chen³⁶, X. R. Chen²⁵, Y. B. Chen^{1,48}, W. S. Cheng^{63C}, G. Cibinetto^{24A}, F. Cossio^{63C}, X. F. Cui³⁷, H. L. Dai^{1,48}, J. P. Dai^{42,g}, X. C. Dai^{1,52}, A. Dbeyssi¹⁵, R. B. de Boer⁴, D. Dedovich²⁹, Z. Y. Deng¹, A. Denig²⁸, I. Denysenko²⁹, M. Destefanis^{63A,63C}, F. De Mori^{63A,63C}, Y. Ding³⁴, C. Dong³⁷, J. Dong^{1,48}, L. Y. Dong^{1,52}, M. Y. Dong^{1,48,52}, S. X. Du⁶⁸, J. Fang^{1,48}, S. S. Fang^{1,52}, Y. Fang¹, R. Farinelli^{24A}, L. Fava^{63B,63C}, F. Feldbauer⁴, G. Felici^{23A}, C. Q. Feng^{60,48}, M. Fritsch⁴, C. D. Fu¹, Y. Fu¹, X. L. Gao^{60,48}, Y. Gao^{38,k}, Y. Gao⁶¹, Y. G. Gao⁶, I. Garzia^{24A,24B}, E. M. Gersabeck⁵⁵, A. Gilman⁵⁶, K. Goetzen¹¹, L. Gong³⁷, W. X. Gong^{1,48}, W. Gradl²⁸, M. Greco^{63A,63C}, L. M. Gu³⁶, M. H. Gu^{1,48}, S. Gu², Y. T. Gu¹³, C. Y. Guan^{1,52}, A. Q. Guo²², L. B. Guo³⁵, R. P. Guo⁴⁰, Y. P. Guo²⁸, Y. P. Guo^{9,h}, A. Guskov²⁹, S. Han⁶⁵, T. T. Han⁴¹, T. Z. Han^{9,h}, X. Q. Hao¹⁶, F. A. Harris⁵³, K. L. He^{1,52}, F. H. Heinsius⁴, T. Held⁴, Y. K. Heng^{1,48,52}, M. Himmelreich^{11,f}, T. Holtmann⁴, Y. R. Hou⁵², Z. L. Hou¹, H. M. Hu^{1,52}, J. F. Hu^{42,g}, T. Hu^{1,48,52}, Y. Hu¹, G. S. Huang^{60,48}, L. Q. Huang⁶¹, X. T. Huang⁴¹, Z. Huang^{38,k}, N. Huesken⁵⁷, T. Hussain⁶², W. Ikegami Andersson⁶⁴, W. Imoehl²², M. Irshad^{60,48}, S. Jaeger⁴, S. Janchiv^{26,j}, Q. Ji¹, Q. P. Ji¹⁶, X. B. Ji^{1,52}, X. L. Ji^{1,48}, H. B. Jiang⁴¹, X. S. Jiang^{1,48,52}, X. Y. Jiang³⁷, J. B. Jiao⁴¹, Z. Jiao¹⁸, S. Jin³⁶, Y. Jin⁵⁴, T. Johansson⁶⁴, N. Kalantar-Nayestanaki³¹, X. S. Kang³⁴, R. Kappert³¹, M. Kavatsyuk³¹, B. C. Ke^{43,1}, I. K. Keshk⁴, A. Khoukaz⁵⁷, P. Kiese²⁸, R. Kiuchi¹, R. Kliemt¹¹, L. Koch³⁰, O. B. Kolcu^{51B,e}, B. Kopf⁴, M. Kuemmel⁴, M. Kuessner⁴, A. Kupsc⁶⁴, M. G. Kurth^{1,52}, W. Kühn³⁰, J. J. Lane⁵⁵, J. S. Lange³⁰, P. Larin¹⁵, L. Lavezzi^{63C}, H. Leithoff²⁸, M. Lellmann²⁸, T. Lenz²⁸, C. Li³⁹, C. H. Li³³, Cheng Li^{60,48}, D. M. Li⁶⁸, F. Li^{1,48}, G. Li¹, H. B. Li^{1,52}, H. J. Li^{9,h}, J. L. Li⁴¹, J. Q. Li⁴, Ke Li¹, L. K. Li¹, Lei Li³, P. L. Li^{60,48}, P. R. Li³², S. Y. Li⁵⁰, W. D. Li^{1,52}, W. G. Li¹, X. H. Li^{60,48}, X. L. Li⁴¹, Z. B. Li⁴⁹, Z. Y. Li⁴⁹, H. Liang^{60,48}, H. Liang^{1,52}, Y. F. Liang⁴⁵, Y. T. Liang²⁵, L. Z. Liao^{1,52}, J. Libby²¹, C. X. Lin⁴⁹, B. Liu^{42,g}, B. J. Liu¹, C. X. Liu¹, D. Liu^{60,48}, D. Y. Liu^{42,g}, F. H. Liu⁴⁴, Fang Liu¹, Feng Liu⁶, H. B. Liu¹³, H. M. Liu^{1,52}, Huanhuan Liu¹, Huihui Liu¹⁷, J. B. Liu^{60,48}, J. Y. Liu^{1,52}, K. Liu¹, K. Y. Liu³⁴, Ke Liu⁶, L. Liu^{60,48}, Q. Liu⁵², S. B. Liu^{60,48}, Shuai Liu⁴⁶, T. Liu^{1,52}, X. Liu³², Y. B. Liu³⁷, Z. A. Liu^{1,48,52}, Z. Q. Liu⁴¹, Y. F. Long^{38,k}, X. C. Lou^{1,48,52}, F. X. Lu¹⁶, H. J. Lu¹⁸, J. D. Lu^{1,52}, J. G. Lu^{1,48}, X. L. Lu¹, Y. Lu¹, Y. P. Lu^{1,48}, C. L. Luo³⁵, M. X. Luo⁶⁷, P. W. Luo⁴⁹, T. Luo^{9,h}, X. L. Luo^{1,48}, S. Lusso^{63C}, X. R. Lyu⁵², F. C. Ma³⁴, H. L. Ma¹, L. L. Ma⁴¹, M. M. Ma^{1,52}, Q. M. Ma¹, R. Q. Ma^{1,52}, R. T. Ma⁵², X. N. Ma³⁷, X. X. Ma^{1,52}, X. Y. Ma^{1,48}, Y. M. Ma⁴¹, F. E. Maas¹⁵, M. Maggiora^{63A,63C}, S. Maldaner²⁸, S. Malde⁵⁸, Q. A. Malik⁶², A. Mangoni^{23B}, Y. J. Mao^{38,k}, Z. P. Mao¹, S. Marcelllo^{63A,63C}, Z. X. Meng⁵⁴, J. G. Messchendorp³¹, G. Mezzadri^{24A}, T. J. Min³⁶, R. E. Mitchell²², X. H. Mo^{1,48,52}, Y. J. Mo⁶, N. Yu. Muchnoi^{10,c}, H. Muramatsu⁵⁶, S. Nakhoul^{11,f}, Y. Nefedov²⁹, F. Nerling^{11,f}, I. B. Nikolaev^{10,c}, Z. Ning^{1,48}, S. Nisar^{8,i}, S. L. Olsen⁵², Q. Ouyang^{1,48,52}, S. Pacetti^{23B,23C}, X. Pan⁴⁶, Y. Pan⁵⁵, A. Pathak¹, P. Patteri^{23A}, M. Pelizaeus⁴, H. P. Peng^{60,48}, K. Peters^{11,f}, J. Pettersson⁶⁴, J. L. Ping³⁵, R. G. Ping^{1,52}, A. Pitka⁴, R. Poling⁵⁶, V. Prasad^{60,48}, H. Qi^{60,48}, H. R. Qi⁵⁰, M. Qi³⁶, T. Y. Qi², S. Qian^{1,48}, W.-B. Qian⁵², Z. Qian⁴⁹, C. F. Qiao⁵², L. Q. Qin¹², X. P. Qin¹³, X. S. Qin⁴, Z. H. Qin^{1,48}, J. F. Qiu¹, S. Q. Qu³⁷, K. H. Rashid⁶², K. Ravindran²¹, C. F. Redmer²⁸, A. Rivetti^{63C}, V. Rodin³¹, M. Rolo^{63C}, G. Rong^{1,52}, Ch. Rosner¹⁵, M. Rump⁵⁷, A. Sarantsev^{29,d}, Y. Schelhaas²⁸, C. Schnier⁴, K. Schoenning⁶⁴, D. C. Shan⁴⁶, W. Shan¹⁹, X. Y. Shan^{60,48}, M. Shao^{60,48}, C. P. Shen², P. X. Shen³⁷, X. Y. Shen^{1,52}, H. C. Shi^{60,48}, R. S. Shi^{1,52}, X. Shi^{1,48}, X. D. Shi^{60,48}, J. J. Song⁴¹, Q. Q. Song^{60,48}, W. M. Song²⁷, Y. X. Song^{38,k}, S. Sosio^{63A,63C}, S. Spataro^{63A,63C}, F. F. Sui⁴¹, G. X. Sun¹, J. F. Sun¹⁶, L. Sun⁶⁵, S. S. Sun^{1,52}, T. Sun^{1,52}, W. Y. Sun³⁵, X. Sun^{20,l}, Y. J. Sun^{60,48}, Y. K. Sun^{60,48}, Y. Z. Sun¹, Z. T. Sun¹, Y. H. Tan⁶⁵, Y. X. Tan^{60,48}, C. J. Tang⁴⁵, G. Y. Tang¹, J. Tang⁴⁹, V. Thoren⁶⁴, B. Tsednee²⁶, I. Uman^{51D}, B. Wang¹, B. L. Wang⁵², C. W. Wang³⁶, D. Y. Wang^{38,k}, H. P. Wang^{1,52}, K. Wang^{1,48}, L. L. Wang¹, M. Wang⁴¹, M. Z. Wang^{38,k}, Meng Wang^{1,52}, W. H. Wang⁶⁵, W. P. Wang^{60,48}, X. Wang^{38,k}, X. F. Wang³², X. L. Wang^{9,h}, Y. Wang⁴⁹, Y. Wang^{60,48}, Y. D. Wang¹⁵, Y. F. Wang^{1,48,52}, Y. Q. Wang¹, Z. Wang^{1,48}, Z. Y. Wang¹, Ziyi Wang⁵², Zongyuan Wang^{1,52}, D. H. Wei¹², P. Weidenkaff²⁸, F. Weidner⁵⁷, S. P. Wen¹, D. J. White⁵⁵, U. Wiedner⁴, G. Wilkinson⁵⁸, M. Wolke⁶⁴, L. Wollenberg⁴, J. F. Wu^{1,52}, L. H. Wu¹, L. J. Wu^{1,52}, X. Wu^{9,h}, Z. Wu^{1,48}, L. Xia^{60,48}, H. Xiao^{9,h}, S. Y. Xiao¹, Y. J. Xiao^{1,52}, Z. J. Xiao³⁵, X. H. Xie^{38,k}, Y. G. Xie^{1,48}, Y. H. Xie⁶, T. Y. Xing^{1,52}, X. A. Xiong^{1,52}, G. F. Xu¹, J. J. Xu³⁶, Q. J. Xu¹⁴, W. Xu^{1,52}, X. P. Xu⁴⁶, L. Yan^{63A,63C}, L. Yan^{9,h}, W. B. Yan^{60,48}, W. C. Yan⁶⁸, Xu Yan⁴⁶, H. J. Yang^{42,g}, H. X. Yang¹, L. Yang⁶⁵,

R. X. Yang^{60,48}, S. L. Yang^{1,52}, Y. H. Yang³⁶, Y. X. Yang¹², Yifan Yang^{1,52}, Zhi Yang²⁵, M. Ye^{1,48}, M. H. Ye⁷,
 J. H. Yin¹, Z. Y. You⁴⁹, B. X. Yu^{1,48,52}, C. X. Yu³⁷, G. Yu^{1,52}, J. S. Yu^{20,l}, T. Yu⁶¹, C. Z. Yuan^{1,52},
 W. Yuan^{63A,63C}, X. Q. Yuan^{38,k}, Y. Yuan¹, Z. Y. Yuan⁴⁹, C. X. Yue³³, A. Yuncu^{51B,a}, A. A. Zafar⁶², Y. Zeng^{20,l},
 B. X. Zhang¹, Guangyi Zhang¹⁶, H. H. Zhang⁴⁹, H. Y. Zhang^{1,48}, J. L. Zhang⁶⁶, J. Q. Zhang⁴, J. W. Zhang^{1,48,52},
 J. Y. Zhang¹, J. Z. Zhang^{1,52}, Jianyu Zhang^{1,52}, Jiawei Zhang^{1,52}, L. Zhang¹, Lei Zhang³⁶, S. Zhang⁴⁹,
 S. F. Zhang³⁶, T. J. Zhang^{42,g}, X. Y. Zhang⁴¹, Y. Zhang⁵⁸, Y. H. Zhang^{1,48}, Y. T. Zhang^{60,48}, Yan Zhang^{60,48},
 Yao Zhang¹, Yi Zhang^{9,h}, Z. H. Zhang⁶, Z. Y. Zhang⁶⁵, G. Zhao¹, J. Zhao³³, J. Y. Zhao^{1,52}, J. Z. Zhao^{1,48},
 Lei Zhao^{60,48}, Ling Zhao¹, M. G. Zhao³⁷, Q. Zhao¹, S. J. Zhao⁶⁸, Y. B. Zhao^{1,48}, Y. X. Zhao²⁵, Z. G. Zhao^{60,48},
 A. Zhemchugov^{29,b}, B. Zheng⁶¹, J. P. Zheng^{1,48}, Y. Zheng^{38,k}, Y. H. Zheng⁵², B. Zhong³⁵, C. Zhong⁶¹,
 L. P. Zhou^{1,52}, Q. Zhou^{1,52}, X. Zhou⁶⁵, X. K. Zhou⁵², X. R. Zhou^{60,48}, A. N. Zhu^{1,52}, J. Zhu³⁷, K. Zhu¹,
 K. J. Zhu^{1,48,52}, S. H. Zhu⁵⁹, W. J. Zhu³⁷, X. L. Zhu⁵⁰, Y. C. Zhu^{60,48}, Z. A. Zhu^{1,52}, B. S. Zou¹, J. H. Zou¹

(BESIII Collaboration)

¹ *Institute of High Energy Physics, Beijing 100049, People's Republic of China*

² *Beihang University, Beijing 100191, People's Republic of China*

³ *Beijing Institute of Petrochemical Technology, Beijing 102617, People's Republic of China*

⁴ *Bochum Ruhr-University, D-44780 Bochum, Germany*

⁵ *Carnegie Mellon University, Pittsburgh, Pennsylvania 15213, USA*

⁶ *Central China Normal University, Wuhan 430079, People's Republic of China*

⁷ *China Center of Advanced Science and Technology, Beijing 100190, People's Republic of China*

⁸ *COMSATS University Islamabad, Lahore Campus, Defence Road, Off Raiwind Road, 54000 Lahore, Pakistan*

⁹ *Fudan University, Shanghai 200443, People's Republic of China*

¹⁰ *G.I. Budker Institute of Nuclear Physics SB RAS (BINP), Novosibirsk 630090, Russia*

¹¹ *GSI Helmholtzcentre for Heavy Ion Research GmbH, D-64291 Darmstadt, Germany*

¹² *Guangxi Normal University, Guilin 541004, People's Republic of China*

¹³ *Guangxi University, Nanning 530004, People's Republic of China*

¹⁴ *Hangzhou Normal University, Hangzhou 310036, People's Republic of China*

¹⁵ *Helmholtz Institute Mainz, Johann-Joachim-Becher-Weg 45, D-55099 Mainz, Germany*

¹⁶ *Henan Normal University, Xinxiang 453007, People's Republic of China*

¹⁷ *Henan University of Science and Technology, Luoyang 471003, People's Republic of China*

¹⁸ *Huangshan College, Huangshan 245000, People's Republic of China*

¹⁹ *Hunan Normal University, Changsha 410081, People's Republic of China*

²⁰ *Hunan University, Changsha 410082, People's Republic of China*

²¹ *Indian Institute of Technology Madras, Chennai 600036, India*

²² *Indiana University, Bloomington, Indiana 47405, USA*

²³ *(A)INFN Laboratori Nazionali di Frascati, I-00044, Frascati, Italy; (B)INFN Sezione di Perugia, I-06100, Perugia, Italy; (C)University of Perugia, I-06100, Perugia, Italy*

²⁴ *(A)INFN Sezione di Ferrara, I-44122, Ferrara, Italy; (B)University of Ferrara, I-44122, Ferrara, Italy*

²⁵ *Institute of Modern Physics, Lanzhou 730000, People's Republic of China*

²⁶ *Institute of Physics and Technology, Peace Ave. 54B, Ulaanbaatar 13330, Mongolia*

²⁷ *Jilin University, Changchun 130012, People's Republic of China*

²⁸ *Johannes Gutenberg University of Mainz, Johann-Joachim-Becher-Weg 45, D-55099 Mainz, Germany*

²⁹ *Joint Institute for Nuclear Research, 141980 Dubna, Moscow region, Russia*

³⁰ *Justus-Liebig-Universitaet Giessen, II. Physikalisches Institut, Heinrich-Buff-Ring 16, D-35392 Giessen, Germany*

³¹ *KVI-CART, University of Groningen, NL-9747 AA Groningen, The Netherlands*

³² *Lanzhou University, Lanzhou 730000, People's Republic of China*

³³ *Liaoning Normal University, Dalian 116029, People's Republic of China*

³⁴ *Liaoning University, Shenyang 110036, People's Republic of China*

³⁵ *Nanjing Normal University, Nanjing 210023, People's Republic of China*

³⁶ *Nanjing University, Nanjing 210093, People's Republic of China*

³⁷ *Nankai University, Tianjin 300071, People's Republic of China*

³⁸ *Peking University, Beijing 100871, People's Republic of China*

³⁹ *Qufu Normal University, Qufu 273165, People's Republic of China*

- ⁴⁰ Shandong Normal University, Jinan 250014, People's Republic of China
- ⁴¹ Shandong University, Jinan 250100, People's Republic of China
- ⁴² Shanghai Jiao Tong University, Shanghai 200240, People's Republic of China
- ⁴³ Shanxi Normal University, Linfen 041004, People's Republic of China
- ⁴⁴ Shanxi University, Taiyuan 030006, People's Republic of China
- ⁴⁵ Sichuan University, Chengdu 610064, People's Republic of China
- ⁴⁶ Soochow University, Suzhou 215006, People's Republic of China
- ⁴⁷ Southeast University, Nanjing 211100, People's Republic of China
- ⁴⁸ State Key Laboratory of Particle Detection and Electronics, Beijing 100049, Hefei 230026, People's Republic of China
- ⁴⁹ Sun Yat-Sen University, Guangzhou 510275, People's Republic of China
- ⁵⁰ Tsinghua University, Beijing 100084, People's Republic of China
- ⁵¹ (A)Ankara University, 06100 Tandogan, Ankara, Turkey; (B)Istanbul Bilgi University, 34060 Eyup, Istanbul, Turkey; (C)Uludag University, 16059 Bursa, Turkey; (D)Near East University, Nicosia, North Cyprus, Mersin 10, Turkey
- ⁵² University of Chinese Academy of Sciences, Beijing 100049, People's Republic of China
- ⁵³ University of Hawaii, Honolulu, Hawaii 96822, USA
- ⁵⁴ University of Jinan, Jinan 250022, People's Republic of China
- ⁵⁵ University of Manchester, Oxford Road, Manchester, M13 9PL, United Kingdom
- ⁵⁶ University of Minnesota, Minneapolis, Minnesota 55455, USA
- ⁵⁷ University of Muenster, Wilhelm-Klemm-Str. 9, 48149 Muenster, Germany
- ⁵⁸ University of Oxford, Keble Rd, Oxford, UK OX13RH
- ⁵⁹ University of Science and Technology Liaoning, Anshan 114051, People's Republic of China
- ⁶⁰ University of Science and Technology of China, Hefei 230026, People's Republic of China
- ⁶¹ University of South China, Hengyang 421001, People's Republic of China
- ⁶² University of the Punjab, Lahore-54590, Pakistan
- ⁶³ (A)University of Turin, I-10125, Turin, Italy; (B)University of Eastern Piedmont, I-15121, Alessandria, Italy; (C)INFN, I-10125, Turin, Italy
- ⁶⁴ Uppsala University, Box 516, SE-75120 Uppsala, Sweden
- ⁶⁵ Wuhan University, Wuhan 430072, People's Republic of China
- ⁶⁶ Xinyang Normal University, Xinyang 464000, People's Republic of China
- ⁶⁷ Zhejiang University, Hangzhou 310027, People's Republic of China
- ⁶⁸ Zhengzhou University, Zhengzhou 450001, People's Republic of China
- ^a Also at Bogazici University, 34342 Istanbul, Turkey
- ^b Also at the Moscow Institute of Physics and Technology, Moscow 141700, Russia
- ^c Also at the Novosibirsk State University, Novosibirsk, 630090, Russia
- ^d Also at the NRC "Kurchatov Institute", PNPI, 188300, Gatchina, Russia
- ^e Also at Istanbul Arel University, 34295 Istanbul, Turkey
- ^f Also at Goethe University Frankfurt, 60323 Frankfurt am Main, Germany
- ^g Also at Key Laboratory for Particle Physics, Astrophysics and Cosmology, Ministry of Education; Shanghai Key Laboratory for Particle Physics and Cosmology; Institute of Nuclear and Particle Physics, Shanghai 200240, People's Republic of China
- ^h Also at Key Laboratory of Nuclear Physics and Ion-beam Application (MOE) and Institute of Modern Physics, Fudan University, Shanghai 200443, People's Republic of China
- ⁱ Also at Harvard University, Department of Physics, Cambridge, MA, 02138, USA
- ^j Currently at: Institute of Physics and Technology, Peace Ave.54B, Ulaanbaatar 13330, Mongolia
- ^k Also at State Key Laboratory of Nuclear Physics and Technology, Peking University, Beijing 100871, People's Republic of China
- ^l School of Physics and Electronics, Hunan University, Changsha 410082, China

We report on a comparison of two possible Λ_c^+ spin hypotheses, $J = \frac{1}{2}$ and $\frac{3}{2}$, via the process $e^+e^- \rightarrow \Lambda_c^+\bar{\Lambda}_c^-$, using the angular distributions of Λ_c^+ decays into pK_S^0 , $\Lambda\pi^+$, $\Sigma^0\pi^+$, and $\Sigma^+\pi^0$. The data were recorded at $\sqrt{s} = 4.6$ GeV with the BESIII detector and correspond to an integrated luminosity of 587 pb⁻¹. The Λ_c^+ spin is determined to be $J = \frac{1}{2}$, with this value favored over the

$\frac{3}{2}$ hypothesis with a significance of 7.98 standard deviations (σ) with a boundary $(7.89 \sim 8.84)\sigma$, corresponding to the observed range of systematic variations.

Since the discovery of Λ_c^+ particle more than 30 years ago [1], many other charmed baryons have been found and studied by experiments [2]. However, the Λ_c^+ spin quantum number has not been determined conclusively until now. The only previous investigation of this property was performed by the NA32 fixed-target experiment [3]. The charmed baryon Λ_c^+ was produced in the process $\pi^- \text{Cu} \rightarrow \Lambda_c^+ \bar{D} X$, where X indicates the other particles produced from the interaction, and the decay $\Lambda_c^+ \rightarrow p K^- \pi^+$ was used to reconstruct the charmed baryon with 160 selected candidate events. The result was compatible with a spin-1/2 assignment, but was not conclusive due to the small sample size.

Currently, the spin of the Λ_c^+ is inferred to be $\frac{1}{2}$ from the naive quark model [4], in which charmed baryons are built from udc quarks, and Λ_c^+ is classified into the mixed-symmetric 20 multiplet with spin-1/2 assignment. Although the quark model works well for the ground state spectroscopy and spin assignment [2], experimental confirmation of the Λ_c^+ spin is essential for testing the quark model prediction. It is also important for understanding the spin and decay properties of doubly charmed baryon states, *e.g.* the newly observed Ξ_{cc}^{++} [5], which decays into final states with Λ_c^+ .

In this Letter, an analysis of the Λ_c^+ spin is performed via the process $e^+e^- \rightarrow \Lambda_c^+ \bar{\Lambda}_c^-$ at the center-of-mass (CM) energy $\sqrt{s} = 4.6$ GeV. The data accumulated with the BESIII [6] detector corresponds to an integrated luminosity of 587 pb^{-1} . We test the spin-1/2 and 3/2 hypotheses based on the angular distributions of the Λ_c^+ decays into $p K_S^0$, $\Lambda \pi^+$, $\Sigma^0 \pi^+$ and $\Sigma^+ \pi^0$. The decays are studied by the single-tag method, *i.e.* either the Λ_c^+ or $\bar{\Lambda}_c^-$ from $e^+e^- \rightarrow \Lambda_c^+ \bar{\Lambda}_c^-$ is reconstructed while the presence of its antiparticle is inferred from kinematics. Throughout the Letter, the charged-conjugation modes are always implied, unless explicitly stated.

The helicity formalism [7, 8] is applied in order to examine the implications of the Λ_c^+ spin hypotheses for the joint angular distribution of the charmed baryon and its daughter particles. Figure 1 shows the helicity frame for the $e^+e^- \rightarrow \Lambda_c^+ \bar{\Lambda}_c^-$ process. The helicity angle, θ_0 , is defined as the polar angle of the Λ_c^+ in the e^+e^- CM system, with the z axis pointing along the positron beam direction. For the Λ_c^+ decay into a spin- $\frac{1}{2}$ baryon (B) and a pseudoscalar meson (P), the z' axis is defined along the direction of the Λ_c^+ , and the y' axis along $\hat{z} \times \hat{z}'$, and the x' axis is determined by $\hat{y}' \times \hat{z}'$. The helicity angle ϕ_1 is defined as the angle between the Λ_c^+ production and decay planes and the helicity angle θ_1 is the angle between the B momentum in the Λ_c^+ rest frame and the z' axis. The helicity angles for the subsequential baryon B decays, (θ_i, ϕ_i) with $i > 2$, can be defined following the same procedure.

The two Λ_c^+ spin hypotheses, $J = \frac{1}{2}$ or $\frac{3}{2}$, are tested

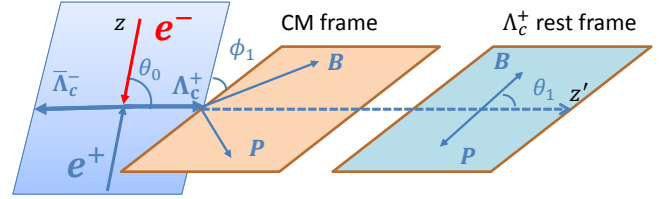


FIG. 1. (color online) Definition of the helicity frame for $e^+e^- \rightarrow \Lambda_c^+ \bar{\Lambda}_c^-$, $\Lambda_c^+ \rightarrow BP$, where B and P denote a spin- $\frac{1}{2}$ baryon and a meson, respectively.

using \mathcal{W}^J , which is the trace of the product of three matrices describing the joint angular distribution of the sequential decays:

$$\mathcal{W}^J = \text{Tr}[\rho_J \cdot \mathcal{T}_J \cdot \mathcal{T}_B]. \quad (1)$$

Here ρ_J is the spin density matrix for a Λ_c^+ baryon produced in the process $e^+e^- \rightarrow \Lambda_c^+ \bar{\Lambda}_c^-$, \mathcal{T}_J is a matrix describing the Λ_c^+ decay to a baryon B and a pseudoscalar meson P , and the baryon B sequentially decaying to the final states is described with a matrix \mathcal{T}_B . The full formulas can be found in Refs [9–11]. As an example, the $\Lambda_c^+ \rightarrow p K_S^0$ decay matrix, \mathcal{T}_B , reduces to the identity matrix, and the joint angular distribution is given by

$$\mathcal{W}^{J=\frac{1}{2}}(\theta_0, \theta_1, \phi_1) \propto 1 + \alpha \cos^2 \theta_0 + \mathcal{P}_\mathcal{T} \sin \theta_1 \sin \phi_1, \quad (2)$$

$$\text{with } \mathcal{P}_\mathcal{T} = \alpha_{[pK_S^0]} \sqrt{1 - \alpha^2} \cos \theta_0 \sin \theta_0 \sin \xi,$$

where α is the angular-distribution parameter of the Λ_c^+ , $\alpha_{[pK_S^0]}$ the asymmetry parameter for the $\Lambda_c^+ \rightarrow p K_S^0$ weak decay and ξ the relative phase between the two independent helicity amplitudes of the produced Λ_c^+ .

The joint angular distribution derived for the spin- $\frac{3}{2}$ hypothesis for $\Lambda_c^+ \rightarrow p K_S^0$ is [10]

$$\begin{aligned} \mathcal{W}^{J=\frac{3}{2}}(\theta_0, \theta_1, \phi_1) &\propto 40r_0^0 - 10\sqrt{3}r_0^2(3 \cos 2\theta_1 + 1) \\ &- 60 [r_1^2 \sin 2\theta_1 \cos \phi_1 + r_2^2 \sin^2 \theta_1 \cos 2\phi_1] \\ &+ \sin \theta_1 \alpha_{[pK_S^0]} [8\sqrt{15}r_{-1}^1 \sin \phi_1 \\ &+ 90r_{-2}^3 \sin 2\theta_1 \sin 2\phi_1 \\ &- 9\sqrt{10}r_{-1}^3(5 \cos 2\theta_1 + 3) \sin \phi_1], \end{aligned} \quad (3)$$

where the real multipole parameters, r_M^L , are defined in terms of the helicity amplitudes for charmed baryon pair production [10].

The BESIII detector is an approximately cylindrically symmetric detector with 93% coverage of the solid angle around the e^+e^- interaction point (IP). The components of the apparatus are a helium-based main drift chamber (MDC), a plastic time-of-flight (TOF) system, a 6240-cell CsI(Tl) crystal electromagnetic calorimeter (EMC), a superconducting solenoid providing a 1.0 T magnetic

field aligned with the beam axis, and a muon counter with resistive plate chambers as the active element. The momentum resolution for charged tracks in the MDC is 0.5% for a transverse momentum of 1 GeV/c. The photon energy resolution in the EMC is 2.5% in the barrel region and 5.0% in the end-cap region for 1 GeV photons. The combined information of the energy deposit in the MDC and the flight time measured by the TOF is used for particle identification (PID) of charged tracks. More details about the design and performance of the BESIII detector are given in Ref. [12].

We use a large Monte Carlo (MC) simulated sample of e^+e^- annihilations to understand background and to estimate the detection efficiencies. The event generation is performed by the KKMC generator [13], taking the beam-energy spread and initial-state radiation (ISR) into account. Inclusive MC samples, consisting of generic $\Lambda_c^+\bar{\Lambda}_c^-$ events, $D_{(s)}^*\bar{D}_{(s)}^* + X$ production [14], ISR production of lower-lying charmonium(-like) ψ states as well as continuum processes $e^+e^- \rightarrow q\bar{q}$ ($q = u, d, s$) are generated for a complete description of the background. The decays are generated using EVTGEN [15] with the decay fractions from Ref. [2] as input. The propagation through the detector and material interactions are simulated by using GEANT4 [16].

The Λ_c^+ candidates are reconstructed from the pK_S^0 , $\Lambda\pi^+$, $\Sigma^+\pi^0$, and $\Sigma^0\pi^+$ final states as done in Refs. [11, 17]. The intermediate states, K_S^0 , Λ , Σ^+ , Σ^0 and π^0 , are reconstructed from the $\pi^+\pi^-$, $p\pi^-$, $p\pi^0$, $\gamma\Lambda$ and $\gamma\gamma$ decays, respectively.

Charged tracks are required to originate from the interaction region, defined by a cylinder with a radius of 1 cm and a distance from the IP along the beam direction of ± 10 cm, except for those charged tracks coming from Λ and K_S^0 decays. The polar angle θ of each track with respect to the beam direction is required to fulfill $|\cos\theta| < 0.93$. Protons are identified by requiring the PID likelihood \mathcal{L} to satisfy $\mathcal{L}(p) > \mathcal{L}(K)$ and $\mathcal{L}(p) > \mathcal{L}(\pi)$, while charged pions are identified using $\mathcal{L}(\pi) > \mathcal{L}(K)$, except for those from Λ and K_S^0 decays.

Clusters in the EMC with no associated charged tracks are identified as photon candidates if the energy deposit in the barrel region ($|\cos\theta| < 0.80$) is larger than 25 MeV or in the endcap region ($0.86 < |\cos\theta| < 0.92$) is larger than 50 MeV. To suppress background from electronic noise and coincidental EMC showers, the difference between the event start time and EMC signal is required to be smaller than 700 ns. The π^0 candidates are reconstructed from photon pairs with an invariant mass, $M(\gamma\gamma)$, which satisfies $115 < M(\gamma\gamma) < 150$ MeV/c². To improve the momentum resolution, a mass-constrained fit to the π^0 nominal mass is applied to the photon pairs and the resulting π^0 energy and momentum is used for the further analysis.

The $\Lambda(K_S^0)$ candidates are formed by combining the final states $p\pi^-(\pi^+\pi^-)$ with a displacement less than 20 cm from the IP along the electron beam direction. The χ^2 of the vertex fit is required to be smaller than

100 and the distance from the IP must be larger than twice the vertex resolution. The momenta of the daughter particles obtained from the fit are used in the further analysis. The charged pions associated with the Λ and K_S^0 candidates are not subjected to any PID requirement, while proton PID is applied in order to improve the signal significance. To select K_S^0 , Λ , Σ^0 , and Σ^+ candidates, we require $487 < M(\pi^+\pi^-) < 511$ MeV/c², $1111 < M(p\pi^-) < 1121$ MeV/c², $1179 < M(\Lambda\gamma) < 1203$ MeV/c², and $1176 < M(p\pi^0) < 1200$ MeV/c², respectively. These requirements correspond to windows of approximately ± 3 standard deviations around the nominal masses. In order to remove pK_S^0 , $K_S^0 \rightarrow \pi^0\pi^0$ background in the $\Sigma^+\pi^0$ sample, the mass of $\pi^0\pi^0$ pair is required to lie outside the range (400, 550) MeV/c².

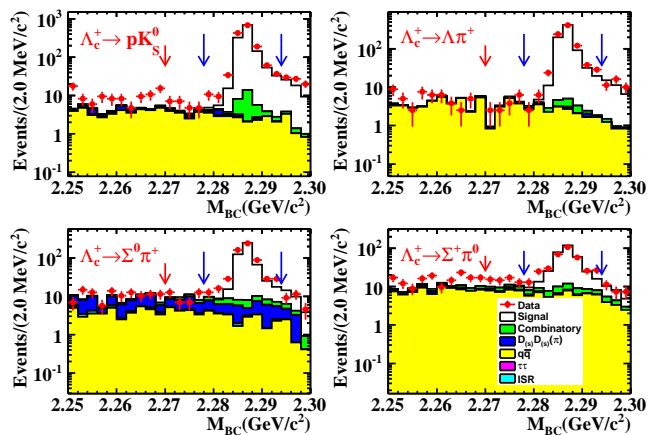


FIG. 2. (color online) The M_{BC} distributions for different decay modes. Points with error bars represent BESIII data, unfilled histograms signal MC samples and shaded histograms MC simulated background. The long vertical arrows indicate the Λ_c^+ mass window, while the sideband region is to the left of the short arrow.

The Λ_c^+ candidates in each decay mode are selected by requiring the beam-constrained mass $M_{BC} \equiv \sqrt{E_{\text{beam}}^2 - p_{\Lambda_c^+}^2}$ to be within the range (2.278, 2.294) GeV/c², where E_{beam} is the beam energy and $p_{\Lambda_c^+}$ is the measured Λ_c^+ momentum in the CM system of the e^+e^- collision. If multiple candidates are found in a single event, we keep the one with the smallest energy difference $|\Delta E|$, where $\Delta E \equiv E_{\Lambda_c^+} - E_{\text{beam}}$ and $E_{\Lambda_c^+}$ is the total measured energy of the Λ_c^+ candidate. To improve the signal purity, ΔE is required to be smaller than three times the resolution of energy difference distribution. The M_{BC} distributions of the different Λ_c^+ decay modes are shown in Fig. 2. The Λ_c^+ candidates appear as a peak at the nominal Λ_c^+ mass whereas the backgrounds, studied in inclusive MC samples, have smooth M_{BC} distributions that are modeled with an Argus function [18]. The background level in the signal region can be estimated from sidebands, defined by M_{BC} values within the range (2.250, 2.270) GeV/c². Table I lists the numbers

of observed (N^{obs}) and normalized background events (N^{bg}) in the Λ_c^+ signal region, where N^{bg} is estimated from the sideband.

TABLE I. Summary of observed (N^{obs}) and normalized background events (N^{bg}) in the Λ_c^+ signal region, where N^{bg} is estimated from the sideband.

Decay	N^{obs}	N^{bg}
$\Lambda_c^+ \rightarrow pK_S^0$	618	25.4
$\bar{\Lambda}_c^- \rightarrow \bar{p}K_S^0$	609	23.6
$\Lambda_c^+ \rightarrow \Lambda\pi^+$	352	10.6
$\bar{\Lambda}_c^- \rightarrow \bar{\Lambda}\pi^-$	344	11.8
$\Lambda_c^+ \rightarrow \Sigma^0\pi^+$	251	26.3
$\bar{\Lambda}_c^- \rightarrow \bar{\Sigma}^0\pi^-$	279	24.2
$\Lambda_c^+ \rightarrow \Sigma^+\pi^0$	192	67.4
$\bar{\Lambda}_c^- \rightarrow \bar{\Sigma}^+\pi^0$	184	52.4

The Λ_c^+ spin- J hypotheses are tested using a likelihood function, which is defined for a given process i as

$$\mathcal{L}_i^J(N^i) = \prod_{k=1}^{N^i} \frac{1}{\mathcal{C}_i^k} \mathcal{W}^J(\theta_0^k, \theta_1^k, \phi_1^k, \dots, \theta_n^k, \phi_n^k), \quad (4)$$

where N^i is the number of events of i th decay mode defined in Table I, $(\theta_0^k, \theta_1^k, \phi_1^k, \dots, \theta_n^k, \phi_n^k)$ are the helicity angles for the k -th event with n -step Λ_c^+ decays, and $\mathcal{C}_i^k = \int \mathcal{W}^J(\theta_0, \theta_1, \phi_1, \dots, \theta_n, \phi_n) d\cos\theta_0 \prod_{m=1}^{m=n} d\cos\theta_m d\phi_m$ is a normalization factor, calculated using a large phase-space MC sample.

The physics parameters are obtained from the joint angular distribution by applying a simultaneous fit to the selected events in the signal region. The background contributions are subtracted from the log-likelihood values using the weighted sideband events. The net log-likelihood for a given process i is defined by

$$\ln \mathcal{L}_i^J = \ln \mathcal{L}_i^J(N_s^i) - \omega^{\text{bg}} \ln \mathcal{L}_i^J(N_b^i), \quad (5)$$

where $N_s^i(N_b^i)$ is the number of selected data (background) events. The background weight, ω^{bg} , is the ratio between the number of background events in the signal region, and the number of sideband events. In estimating the background weight, its line shape is taken as an Argus function.

The MINUIT [19] package is used to minimize the objective function, $S = -\sum_i \ln \mathcal{L}_i^J$, in the simultaneous fit to the pK_S^0 , $\Lambda\pi^+$, $\Sigma^0\pi^+$, and $\Sigma^+\pi^0$ decay modes. The decay asymmetry parameters for the spin- $\frac{1}{2}$ hypothesis, *e.g.* $\alpha_{[pK_S^0]}$ in Eq. (2) are constrained in the range $[-1, 1]$ in the simultaneous fit. For the spin- $\frac{3}{2}$ hypothesis, the asymmetry parameters in the fit are constrained in the physical region [20] for each mode, *i.e.* $-\frac{1}{3} \leq \alpha_{[BP]} \leq \frac{1}{3}$. The relative phase between the helicity amplitudes are fixed to the expected values near threshold [10], whereas the moduli of the helicity amplitudes in r_M^L are obtained from the fit. The minimum log-likelihood, given by $-\sum_i \ln \mathcal{L}_i^J$, is determined to be -45.18 for the spin- $\frac{1}{2}$

hypothesis and -21.50 for the spin- $\frac{3}{2}$ hypothesis. Hence, our data favors the spin- $\frac{1}{2}$ hypothesis.

The distribution of $\langle \sin 2\theta_1 \cos \phi_1 \rangle$ moment, an average observed in each bin, is a useful observable to illustrate the different behaviour expected for the two hypotheses. Figure 3 shows the first moment of the $\langle \sin 2\theta_1 \cos \phi_1 \rangle$ distribution under the two spin hypotheses for the all-mode-combined events, and the projections of the two fits suggest that the data favor the spin- $\frac{1}{2}$ to the spin- $\frac{3}{2}$ hypothesis.

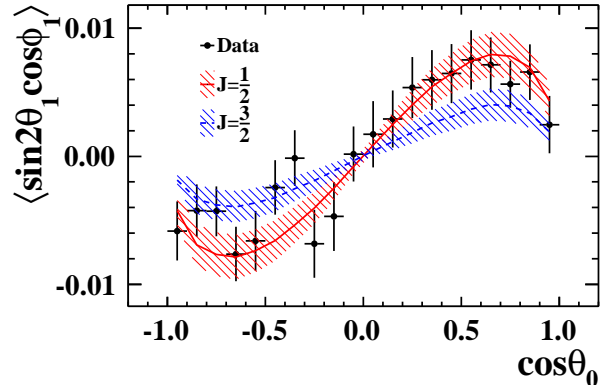


FIG. 3. (color online) The moments $\langle \sin 2\theta_1 \cos \phi_1 \rangle$ as a function of $\cos \theta_0$. Points with error bars represent data from all four Λ_c^+ decay candidates, where the background contribution has been subtracted. The red solid curve shows the fitted result of the spin- $\frac{1}{2}$ hypothesis, whereas the blue dashed curve shows that of the spin- $\frac{3}{2}$ hypothesis. The bands represent the fit uncertainty due to statistical uncertainties.

The significance for the spin- $\frac{1}{2}$ assignment is determined using the Wilks theorem [21] with the maximized likelihood values for two trials. One trial is describing the data events with a linear combination of $\mathcal{W}^{J=1/2}$ and $\mathcal{W}^{J=3/2}$, and the other with $\mathcal{W}^{J=3/2}$. The change of maximized likelihood, $-\Delta(2 \ln L)$, is 90.4 corresponding the change of number of degree of freedom 9. Hence the statistical significance for the spin- $\frac{1}{2}$ assignment is determined to be 7.98σ over the spin- $\frac{3}{2}$ assignment.

The significance to accept the spin- $\frac{1}{2}$ hypothesis over the spin- $\frac{3}{2}$ hypothesis can be affected by the systematic sources listed in Table II. We estimate these systematic variations with the same Wilks theorem that was used for the likelihood ratio. The results are listed in Table II.

The efficiencies of the tracking and PID for charged tracks and their dependence on transverse momentum and polar angle are measured using a control data sample $J/\psi \rightarrow p\bar{p}\pi^+\pi^-$ decays [22]. The uncertainties associated with the detection efficiency of the radiative photon in $\Sigma^0 \rightarrow \gamma\Lambda$ decays are assessed with a control sample of $J/\psi \rightarrow \pi^+\pi^-\pi^0, \pi^0 \rightarrow \gamma\gamma$ decays. The efficiency differences between data and MC simulations are determined to be 0.5% and 1.5% in the barrel and endcap re-

TABLE II. Systematic uncertainties for estimating the significance of spin- $\frac{1}{2}$ versus the spin- $\frac{3}{2}$ hypothesis determined with the Wilks theorem.

Source	Significance
Nominal fit	7.98 σ
Tracks and PID	
Photon	8.84 σ
π^0	(combined)
Λ	
Sideband window	(8.03, 7.79) σ
Signal window	(7.93, 8.32) σ
ΔE	(7.91, 7.95) σ
ω^{bg}	(7.99, 8.13) σ
$M_{\pi^0\pi^0}$ veto	(7.89, 8.19) σ

gion, respectively [23]. The difference between data and MC simulation of the π^0 reconstruction efficiency in the $\Lambda_c^+ \rightarrow \Sigma^+\pi^0$ decay, and its dependence on momentum, is studied using the processes $\psi(3686) \rightarrow \pi^0\pi^0 J/\psi$ and $e^+e^- \rightarrow \pi^0\omega$ at $\sqrt{s} = 3773$ MeV. The Λ reconstruction efficiency is studied as a function of momentum and polar angle in the reaction $\Lambda_c^+ \rightarrow \Lambda + X$ [24]. To take into account the correlations between the different sources of correction and uncertainty, we perform an overall weighting of MC events in the fit according to these efficiency corrections. We determine the significance of spin- $\frac{1}{2}$ hypothesis to be 8.84 σ with this approach.

The systematic uncertainties due to the event selection criteria of the ΔE , signal and sideband events are estimated by varying their requirements by 1 MeV. The uncertainty due to the $M_{\pi^0\pi^0}$ rejection criterion in the $\Lambda_c^+ \rightarrow \Sigma^+\pi^0$ channel is checked with a tight and loose requirement, *ie.*, $M_{\pi^0\pi^0} \in [0.42, 0.53]$ GeV/ c^2 and $[0.38, 0.57]$ GeV/ c^2 . The potential bias due to the sideband scale factor, ω^{bg} , is evaluated through varying the parameters by 1 σ for the Argus fit function. The ranges of significance estimation are given in Table II. The resulting significance comparing the two hypothesis tests are found to be 7.98 σ with a systematic boundary (7.89 \sim 8.84) σ , where the uncertainties correspond to the smallest and largest values listed in Table II.

In conclusion, we have compared the two spin hypotheses $\frac{1}{2}$ and $\frac{3}{2}$ for the Λ_c^+ baryon by studying the process $e^+e^- \rightarrow \Lambda_c^+\bar{\Lambda}_c^-$, using 587 pb $^{-1}$ of BESIII data collected at $\sqrt{s} = 4.6$ GeV. The analysis considered the joint angular distribution of the production and decay modes $\Lambda_c^+ \rightarrow pK_S^0$, $\Lambda\pi^+$, $\Sigma^0\pi^+$ and $\Sigma^+\pi^0$. We found that the spin of $\frac{1}{2}$ hypothesis is preferred over the $\frac{3}{2}$ with a significance of 7.98 σ with a systematic boundary (7.89 \sim 8.84) σ . Hence, we conclude the spin of the Λ_c^+ baryon to be $\frac{1}{2}$, consistent with the expectation of the naive quark model. Since the Λ_c^+ is the lightest charmed baryon, this experimental determination of its spin is also a cornerstone in the extraction of the properties of heavier charmed and beauty baryons whose decay chains include this particle.

The BESIII collaboration thanks the staff of BEPCII and the IHEP computing center for their strong support. This work is supported in part by National Key Basic Research Program of China under Contract No. 2015CB856700, 2020YFA0406400; National Natural Science Foundation of China (NSFC) under Contracts Nos. 11875262, 11625523, 11635010, 11735014, 11822506, 11835012, 11935015, 11935016, 11935018, 11961141012; the Chinese Academy of Sciences (CAS) Large-Scale Scientific Facility Program; Joint Large-Scale Scientific Facility Funds of the NSFC and CAS under Contracts Nos. U1732263, U1832207; CAS Key Research Program of Frontier Sciences under Contracts Nos. QYZDJ-SSW-SLH003, QYZDJ-SSW-SLH040; 100 Talents Program of CAS; INPAC and Shanghai Key Laboratory for Particle Physics and Cosmology; ERC under Contract No. 758462; German Research Foundation DFG under Contracts Nos. Collaborative Research Center CRC 1044, FOR 2359; Istituto Nazionale di Fisica Nucleare, Italy; Ministry of Development of Turkey under Contract No. DPT2006K-120470; National Science and Technology fund; STFC (United Kingdom); The Knut and Alice Wallenberg Foundation (Sweden) under Contract No. 2016.0157; The Royal Society, UK under Contracts Nos. DH140054, DH160214; The Swedish Research Council; U. S. Department of Energy under Contracts Nos. DE-FG02-05ER41374, DE-SC-0012069; Olle Engkvist Foundation under Contract No. 200-0605.

-
- [1] J. C. Anjos *et al.* (Tagged Photon Spectrometer Collaboration), Phys. Rev. Lett. **60**, 1379 (1988).
[2] P. A. Zyla *et al.* (Particle Data Group), Prog. Theor. Exp. Phys. **2020**, 083C01 (2020).
[3] M. Jezabek, K. Rybicki and R. Rylko, Phys. Lett. B **286**, 175 (1992).
[4] M. Gell-Mann, Phys. Lett. **8**, 214 (1964).
[5] R. Aaij *et al.* (LHCb Collaboration), Phys. Rev. Lett. **119**, 112001 (2017).
[6] M. Ablikim *et al.* (BESIII Collaboration), Chin. Phys. C **44**, no.4, 040001 (2020).
[7] M. Jacob and G. C. Wick, Ann. Phys. (Paris) **7**, 404 (1959).
[8] S. U. Chung, CERN Yellow Report No. CERN 71-8 (1971).
[9] Hong Chen and Rong-Gang Ping, Phys. Rev. D **99**, 114027 (2019).
[10] E. Perotti, G. Fäldt, A. Kupsc, S. Leupold and J. J. Song, Phys. Rev. D **99**, 056008 (2019).
[11] M. Ablikim *et al.* (BESIII Collaboration), Phys. Rev. D **100**, 072004 (2019).
[12] M. Ablikim *et al.*, Nucl. Instrum. Meth. Phys. Res. Sect. A **614**, 345 (2010).
[13] S. Jadach *et al.*, Phys. Rev. D **63**, 113009 (2001).

- [14] N. Brambilla *et al.*, Eur. Phys. J. C **71**, 1534 (2011).
- [15] D. J. Lange, Nucl. Instrum. Meth. A **462**, 152 (2001); R. G. Ping, Chin. Phys. C **32**, 599 (2008).
- [16] S. Agostinelli *et al.* (GEANT Collaboration), Nucl. Instrum. Meth. A **506**, 250 (2003); J. Allison *et al.*, IEEE Trans. Nucl. Sci. **53**, 270 (2006).
- [17] M. Ablikim *et al.* (BESIII Collaboration), Phys. Rev. Lett. **116**, 052001 (2016).
- [18] H. Albrecht *et al.* (ARGUS Collaboration), Phy. Lett. B **241**, 278 (1990).
- [19] F. James, CERN Program Library Long Writeup D **506** (1998).
- [20] T. D. Lee and C. N. Yang, Phys. Rev. **109**, 1755 (1958).
- [21] S. S. Wilks, Ann. Math. Stat. **9**, 60 (1938).
- [22] M. Ablikim *et al.* (BESIII Collaboration), Phys. Rev. D **89**, 071101 (2014).
- [23] M. Ablikim *et al.* (BESIII Collaboration), Phys. Rev. D **92**, 052003(R) (2015); **93**, 039906(E) (2015).
- [24] M. Ablikim *et al.* (BESIII Collaboration), Phys. Rev. Lett. **121**, 062003 (2018).